1994A&A...283..435K

Astron. Astrophys. 283, 435–440 (1994)

ASTRONOMY
AND
ASTROPHYSICS

Observations from the gamma-ray burst experiment onboard the SROSS-C satellite

K. Kasturirangan, T.M.K. Marar, V.N. Padmini, N.L. Prasad, U.R. Rao and S. Seetha

ISRO Satellite Centre, Airport Road, Vimanapura PO, Bangalore 560 017, India

Received 26 February 1993 / Accepted 22 August 1993

Abstract. A gamma-ray burst (GRB) experiment was launched onboard the SROSS-C satellite on May 20, 1992. The experiment covered an energy domain of 20 keV–3 MeV and had a time resolution of 2 ms. It operated satisfactorily till the re-entry of the satellite on July 14, 1992. The experiment recorded high resolution temporal and spectral data on a few interesting events. Details of three of them and their preliminary analysis are presented. Of these three events the one which was detected on June 29, in particular, exhibits strong oscillations with a pronounced periodicity of 237.03 ± 0.5 ms. Possible explanations for this fast variability are explored in this paper.

Key words: space vehicles – gamma rays: bursts – gamma rays: observations

1. Introduction

Although the discovery of cosmic gamma ray bursts (GRBs) was first reported nearly two decades ago (Klebesadel et al. 1973), the identity of the burst sources and the processes of production of these bursts of high energy gamma rays remain as major unsolved puzzles in high energy astrophysics. Recent reviews on gamma ray bursts by Liang & Petrosian (1986), Hurley (1988) and Higdon & Lingenfelter (1990) provide a critical assessment of the available data and their interpretation. Several hundred bursts have so far been recorded over the years by a variety of instruments flown on a number of spacecrafts forming an interplanetary network for the detection and measurement of gamma ray bursts. Despite extensive searches in the radio, infrared, optical, X-ray and gamma ray wavelengths of the electromagnetic spectrum for the detection of candidate objects within the error boxes provided by the interplanetary network for a number of GRB events, identification of the quiescent counterparts of GRB sources has so far been unsuccessful. The search and identification of these events therefore continue to be a major effort in observational astrophysics.

Presently, the Compton Gamma Ray Observatory (CGRO) in a near-earth orbit, the GRANAT satellite in a highly eccentric orbit around the earth and the Ulysses spacecraft close to Jupiter, carry onboard GRB detectors of varying sensitivity and sophistication. The BATSE instrument on CGRO provides a sensitivity for the detection of bursts of fluence greater than about 10^{-7} erg cm^{-2} and can determine directions of bright bursts to an accuracy of about a few square degrees. Over 500 gamma ray bursts have been recorded to date using BATSE. The most astounding result from this data is that the angular distribution of GRB sources is found to be isotropic, with no concentration towards the galactic plane, or in the directions of any other nearby galaxy or cluster of galaxies (Meegan et al. 1992). In addition, the integrated brightness distribution of these sources shows a depletion of weaker bursts with respect to the expected $-3/2$ power law. This would indicate that the spatial distribution of the sources, in addition to being isotropic, is also confined. These findings have important consequences to our understanding of the nature of GRB sources, their distances and energetics. They have led to extensions, revisions and/or new hypotheses of galactic, extragalactic and cosmological models.

CGRO is operating in a low earth orbit, and hence a large part of the sky will always be occulted by the earth. The sky coverage can be improved by having a few more GRB detectors in near earth orbit. This will offer additional inputs for the localisation of bursts by means of an effective interplanetary network of detectors. With the above motivation, a gamma ray burst experiment was designed and launched onboard the Indian SROSS-C satellite. Its primary scientific objectives included:

(a) monitoring of GRBs in the energy range 20 keV–3 MeV,

(b) determination of the intensity variation with high time resolution (2 ms around the peak of the burst); to search for periodicities in the incident radiation and

---

Send offprint requests to: T.M.K. Marar

© European Southern Observatory • Provided by the NASA Astrophysics Data System

1994A&A...283..435K

(c) determination of the temporal evolution of the energy spectra with a 124 channel pulse height analyser to search for cyclotron lines and features in the energy range 20–100 keV and possible redshifted annihilation radiation in the energy range 400–500 keV.

The GRB instrument was launched onboard the Indian Stretched Rohini Satellite Series (SROSS)-C on May 20, 1992 by an Augmented Satellite Launch Vehicle (ASLV). The SROSS-C achieved an elliptical orbit with an apogee of 433 km and a perigee of 268 km and had an inclination of 45.6°. It was spin stabilised, with a spin rate of 5.7 rpm and the spin axis was maintained parallel to the negative orbit normal by a magnetic torquer. SROSS-C re-entered the atmosphere on July 14 after completing 888 orbits. The GRB experiment on SROSS-C operated satisfactorily from the time of its initial switch-ON on May 25 till the last tracked orbit of the satellite. In this paper we present details of the experiment, the observations conducted and a few interesting events recorded by the experiment.

2. Instrumentation

The GRB instrumentation consists of a main and a redundant CsI(Na) scintillation detector of 76 mm and 37 mm diameter, each having a thickness of 12.5 mm and optically coupled to EMI 9758NA and RCA 7151Q photomultiplier tubes (PMT) respectively. Separate high voltage DC–DC converters are used to bias the PMTs. A RCA CDP 1802 microprocessor based instrumentation is employed for collecting and processing the temporal and spectral data. When the 100–1024 keV count rate exceeds a preset 256 or 1024 ms threshold rate, the processor recognises it as a burst, freezes 65 s of temporal and 2 s of spectral data prior to this trigger time in a circulating memory and stores detailed spectral and temporal information on the burst for the ensuing 16 s and 204 s respectively. In addition, the onboard time and several house keeping parameters are also stored. The trigger thresholds can be changed by data commands from ground. A permanently mounted Cd^{109} (88 keV) radioactive source is used for energy calibration.

The low resolution data of the experiment consists of two energy channels (20–100 keV and 100–1024 keV) from 65 s prior to burst detection to 204 s after burst detection with an integration time of 256 ms. In addition, the (20–1024 keV) rates are recorded with a high temporal resolution of 2 ms from $T_0 - 1$ to $T_0 + 1$ s, where T_0 is the trigger time. From $T_0 + 1$ to $T_0 + 8$ s, the above rates are measured with a time resolution of 16 ms.

Energy spectral measurements are conducted with a 124 channel pulse height analyser. The latter has a 4 keV per channel nominal resolution from 20 to 256 keV, 8 keV/channel from 256 to 512 keV and 16 keV/channel from 512 to 1024 keV. Four preburst spectra (in a circulating memory) and 32 post-burst spectra are stored for every burst, each spectrum being taken for a duration of 512 ms.

The detectors were calibrated on ground using different energy sources and at different temperatures in vacuum. The measured energy resolution of the main detector at 88 keV was $21.8 \pm 5\%$ at a temperature of 293 K. The time of a GRB event, when registered, can be determined to an accuracy of ± 30 ms using a correlation between onboard and ground based clocks. Further details may be obtained in Marar et al. (1993).

In order to switch-off the high voltages to the PMTs when the satellite passes over the intense charged particle radiation zones in the South Atlantic Anomaly (SAA) region and certain high latitude regions, the count rate in the (1–3) MeV channel is monitored. When the rate exceeds a preset threshold (which can be changed by ground command), the HV is turned off for the ensuing 20 min.

Different modes of operation of the experiment enable calibration, background radiation mapping and detailed temporal and spectral studies of any specific region of a given orbit. Further details of the instrumentation are available in Marar et al. (1993).

3. Observations and results

During the life of the SROSS-C satellite in orbit, a total of 53 triggers were recorded by the GRB payload. As is to be expected, a large number of triggers, were false triggers, recorded when the satellite passed through high latitude radiation zones, particularly around 40–45.6° south/north latitudes i.e., over the north-pacific, south-pacific and south-Australian zones, where intense trapped radiation-belt particles are known to exist. Detection of false triggers occurs when the number of charged particles that deposited energy between 0.1 and 1 MeV exceeded either the 256 or 1024 ms trigger threshold, while the 1–3 MeV rate remained less than the South Atlantic Anomaly detection threshold. This is the expected scenario for a genuine gamma ray burst also. In high latitudes the 1–3 MeV flux of particles is frequently low, leading to a situation conducive for a false trigger in the system. In the SAA region, however, the flux of 1–3 MeV particles is large and hence the SAA detection logic would switch the HV "off", whenever the satellite passed through this region. The performance of the payload under the above situations was found to be reliable and always consistent. In the background mode of operation of the experiment, the count rates and spectra taken over equatorial latitudes were consistent with one another. The redundant detector which was operated towards the fag end of the mission also revealed count rates and spectra consistent with those obtained using the main detector.

Of the 53 events registered by our instrument we list in Table 1, 8 events which we believe to be interesting eventhough they again occur at latitudes of 40–45.6°. Of these, the event registered in orbit no. 534, has been corroborated by CGRO to be a magnetospheric event based on timing of the event (Kouveliotou, private communication). Since our

© European Southern Observatory • Provided by the NASA Astrophysics Data System

1994A&A...283..435K

Table 1

Orbit Ref. No.	Event date	Time in UT (hh mm ss)	Position of the satellite		
			Latitude (deg)	Longitude (deg)	Altitude (km)
331	June 09	20 39 02.33	43.7	− 102.3	246
377	June 12	18 06 48.19	43.6	− 84.9	250
436	June 16	11 54 02.00	− 46.0	− 175.0	364
502	June 20	15 13 45.51	− 46.0	+ 105.0	332
534	June 22	15 10 22.86	− 35.7	+ 48.8	284
597	June 26	13 42 53.76	− 39.0	+ 50.0	263
640	June 29	06 17 44.89	− 44.5	− 158.0	279
864	July 13	03 20 10.0	− 44.0	+ 107.0	195

detector does not have an anticoincidence shield, we cannot distinguish clearly true gamma ray events from particle events. When the instrument is triggered during its passage through a particle belt, we expect the count rate to increase in a few tens of seconds and then saturate. On the other hand, a GRB event will have typical rise times ranging from a few milliseconds to a few seconds, and their durations are anywhere between fraction of a second to a few hundreds of seconds. We have therefore used this criteria to further elaborate on only 3 of the events out of those listed in the Table 1, since they best mimic the characteristics of GRBs.

The burst recorded on June 29 at 06:17:45 UT is particularly interesting. The (20–1024 keV) light curve of the event from $T_0 - 1$ to $T_0 + 8$ s, where T_0 is the burst trigger time, is shown in Fig. 1a. Here the integration time is 16 ms. Figure 1b shows the data from $T_0 - 1$ to $T_0 + 1$ s at the highest resolution of 2 ms available from the experiment. Visual inspection of the figures clearly reveals the presence of strong oscillations in the incident radiation at a period of about 240 ms. The SROSS-C spin period is $\sim$ 10.6 s and hence its effect on the fast modulation at 240 ms is negligible. The damped oscillations are visible for a duration of at least 12 cycles. The rise time of this event is about 150 ms. Its total duration is about 60 s. At the peak of the event the counting rate was about 40 sigma above the background level.

Figures 1c and 1d show the 20–100 and 100–1024 keV count rates for the duration of the event. From $T_0 + 1$ to $T_0 + 8$ s the integration time is 16 ms and each bin has a capacity of 127 counts. Hence the light curve does not saturate here. From $T_0 + 8$ s onwards the integration time is 256 ms and the bin capacity is still 127 counts only. Hence one can see the count rates saturating from $T_0 + 8$ s to about $T_0 + 30$ s when the rate in this particular event reduced to 127 counts in 256 ms. Figure 2 shows the preliminary background subtracted raw count rate spectrum of the event.

We have subjected the oscillatory part of the data spanning 4.3 s to a Fourier transform analysis. The amplitude spectrum obtained is shown in Fig. 3. The period determined from the analysis corresponds to 237.03 ± 0.5 ms. The Fourier transform of the data from $T_0 + 4$ to $T_0 + 8$ s did not reveal any periodicity.

Since the event occurred when the satellite was located at a latitude of $-44.5°$, it can be caused by the presence of precipitating electrons from the trapped radiation belt around the earth. In this case one has to conjecture that our detector encountered at least 12 bunches of particles, equally spaced at distances of about 1.5 km separation from one another. Intense precipitation of energetic electrons from the geomagnetic field during magnetic storms with multiple periods in the range of a fraction of a second to a few seconds has been reported in literature (Winckler et al. 1962). The Sun was occulted by the earth as seen by the SROSS-C satellite at the time when this event occurred. However, we may mention that on June 29 the Sun was very active and several solar hard X-ray bursts were detected by the GRB experiment on Ulysses satellite (Kevin Hurley, private communication) and the planetary magnetic index was about 38 (DRK Rao, Indian Institute of Geomagnetism, private communication). Therefore the magnetospheric precipitation of electrons is a very likely cause for this event. The event is however unique in that its power spectrum reveals a single frequency. The absence of periodicity in the 4–8 s region of the data could then be attributed to the movement of the spacecraft out of the region containing electrons oscillating between conjugate points in the geomagnetic field.

The striking coincidence of the observed 237.03 ms period with that of the Geminga pulsar (237.09 ms) (Halpern & Holt 1992), the second brightest gamma ray source in the sky at high energies, is indeed surprising. At the time of this event Geminga was below the horizon as seen from our satellite and hence, unless the radiation is so intense that the fluorescence from the earth's atmosphere becomes detectable, the matching between the two periods may merely be a chance coincidence. Moreover the BATSE instrument on the Compton Gamma Ray Observatory and the Ulysses GRB experiment, have not detected this event (Chryssa Kouveliotou and Kevin Hurley, private communication). This would argue against an association between

© European Southern Observatory • Provided by the NASA Astrophysics Data System

1994A&A...283..435K

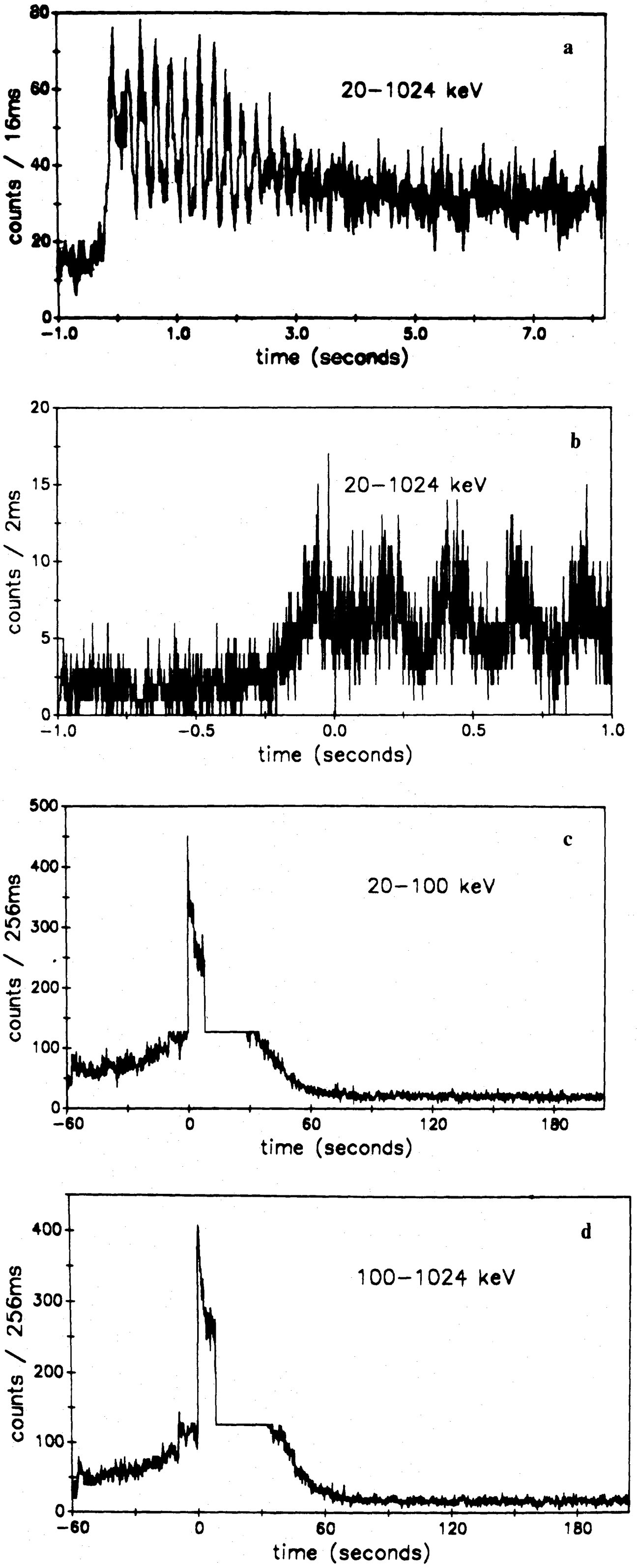

Fig. 1a–d. Temporal profiles of June 29, 6 : 17 : 45 UT event for different durations with respect to the event detection time T_0. **a** $T_0 - 1$ to $T_0 + 8$ s at 16 ms resolution. **b** $T_0 - 1$ to $T_0 - 1$ s at 2 ms resolution. **c** $T_0 - 60$ to $T_0 + 204$ s at 256 ms resolution 20–100 keV data. **d** $T_0 - 60$ to $T_0 + 204$ s at 256 ms resolution, 100–1024 keV data

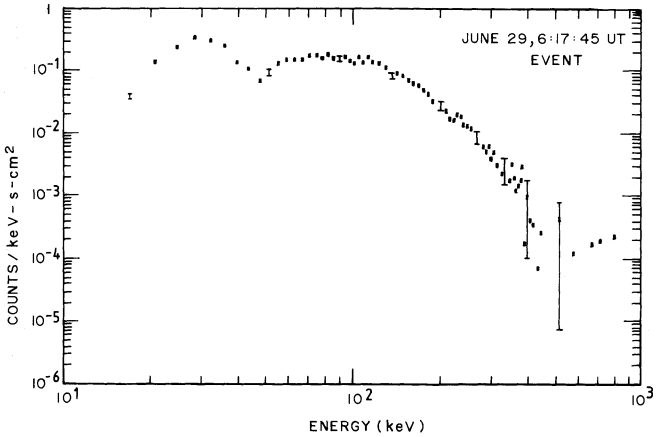

Fig. 2. Background subtracted raw energy spectrum of the June 29 event. One sigma statistical errors of flux at typical energies are indicated in the figure

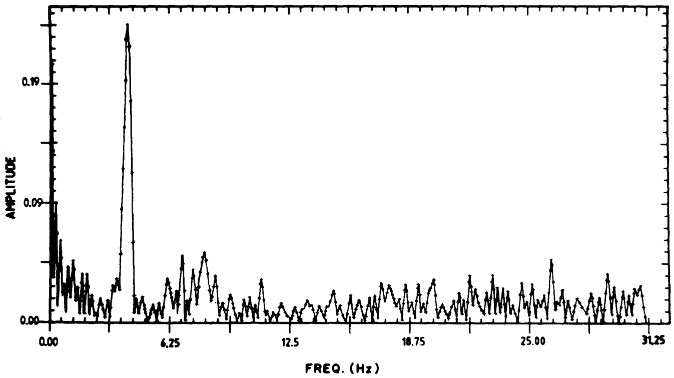

Fig. 3. The amplitude spectrum of the June 29 event obtained by subjecting the data to Fourier transform

this event and the Geminga pulsar since the more sensitive BATSE instrument should have invariably seen either the direct radiation or the fluorescence from the earth's atmosphere, independent of the position of CGRO in its orbit.

We may also mention that the radio pulsars, PSR 1922 + 20 (pulse period = 237.79 ms) and PSR 1719 − 37 (pulse period = 236.17 ms) (Manchester & Taylor 1981) have periods closest to the observed period of 237.03 ms of our event. The angles between the detector normal and the above sources at the time of the event were 74° and 9.5° respectively and hence both pulsars were in the field of view of the detector. However since these radio pulsars have not been identified as X-ray/gamma ray sources, the matching of the observed period with that of the pulsars may again be a coincidence.

A third and less likely possibility is that of the detection of a poorly shielded nuclear powered satellite by our instrument. The origin of the 237.03 ms period, would then demand an unusually and therefore unlikely fast spin rate for the satellite if one assumes that the modulation results from the shielding of the nuclear reactor by the satellite

© European Southern Observatory • Provided by the NASA Astrophysics Data System

1994A&A...283..435K

body. The asymmetric nature of the time history of the event also argues against this hypothesis.

To summarise, the event detected by us on June 29 is unique due to the presence of strong periodic oscillations with a period of 237.03 ms. This event will acquire great significance if the mechanism for the production of the above oscillations is understood in terms of physical processes.

The second event registered on June 12 at 18:06:48 UT is shown in Fig. 4a and 4b. The temporal profile of the 100–1024 keV counting rate from $T_0 - 10$ to $T_0 + 10$ s, plotted at 256 ms resolution, is shown in Fig. 4a. This near symmetric event had a rise time of about 512 ms and a duration of 2.5 s. The temporal profile of the 20–1024 keV countrate is plotted at a resolution of 16 ms in Fig. 4b. The initial burst followed by a few spikes of shorter duration and decreasing intensity is characteristic of many celestial gamma ray bursts. The counting rate at the peak of the burst is about 270 counts s^{-1} in the energy range 20–100 keV and about 210 counts s^{-1} in the range 100–1024 keV. The fluence of this event is about 5 10^{-6} erg cm^{-2}.

The temporal profiles of the burst candidate detected on June 16, 1992 at 11:54:02 UT are shown in Figs. 5a and 5b. In this case one observes before the trigger a precursor which is followed by five to six bursts of radiation. The 20–100 keV flux has a rise time of 5 s. The main pulse lasts for 12–13 s while the event itself lasts about 78 s. The peak counting rate from 20 to 100 keV is about 400 count s^{-1} and from 100–1024 keV 290 count s^{-1}.

At the times of the above two events, BATSE on CGRO had no recording of data due to the failure of the onboard tape recorders (Kouveliotou, private communication). Ulysses did not record a trigger at these times (Kevin Hurley, private communication). Since non-detection by Ulysses could very well have been due to source occultation by the satellite body, the localisation of these events is not possible (that is, in the absence of detection by CGRO or at least two satellites).

4. Conclusions

The gamma ray burst experiment on the Indian SROSS-C satellite operated satisfactorily during May 25–July 14, 1992. It recorded a few GRB candidate events in addition to several high latitude false triggers caused by precipitating electrons from the earth's trapped radiation belts. One of the events, recorded on June 29, is unique in its temporal profile in that it showed damped oscillations with a period of 237 ms. The event recorded on June 16 has a temporal profile similar to that of classical gamma ray bursts.

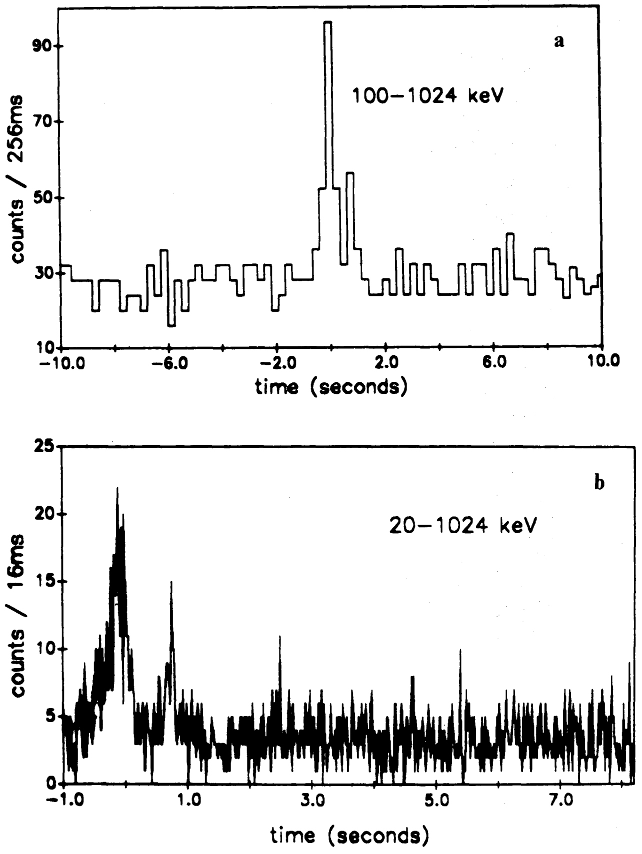

Fig. 4a and b. Temporal profiles of June 12, 18:06:48 UT event for different durations with respect to the event detection time T_0, **a** $T_0 - 10$ to $T_0 + 10$ s, 256 ms resolution 100–1024 keV. **b** $T_0 - 1$ to $T_0 + 8$ s, 16 ms resolution 20–1024 keV

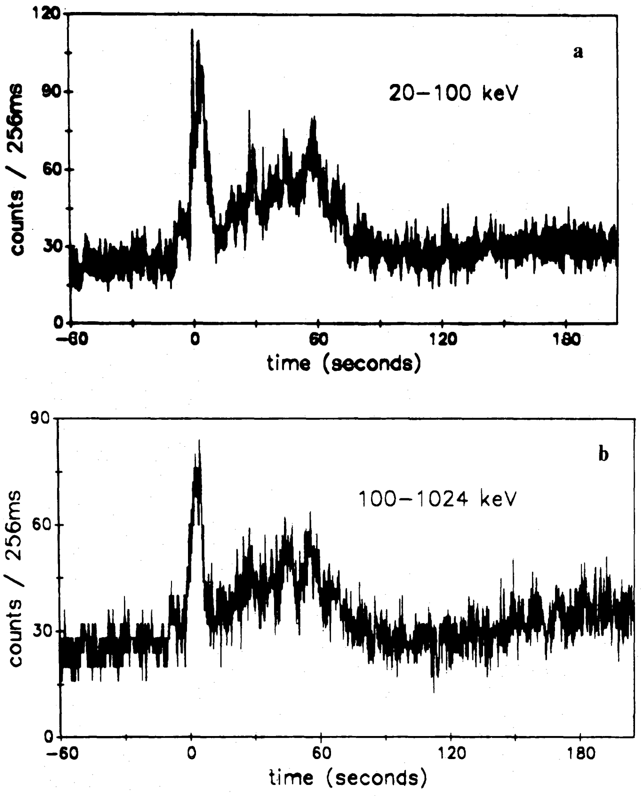

Fig. 5a and b. Temporal profiles of June 16, 11:54:02 UT event in 2 energy channels. **a** $T_0 - 60$ to $T_0 + 204$ s, 256 ms resolution 20–100 keV. **b** $T_0 - 60$ to $T_0 + 204$ s, 256 ms resolution 100–1024 keV

© European Southern Observatory • Provided by the NASA Astrophysics Data System

1994A&A...283..435K

Acknowledgements. The authors are grateful for the invaluable support given by the Project Engineer of the experiment Mr. M. Ramakrishna Sharma and his team of electronics engineers. The authors thank Ms. Padma for her cheerful secretarial assistance in the preparation of this paper. They also thank the referees for many useful suggestions that helped improve the paper.

References

Halpern J.P., Holt S.S., 1992, Nat 357, 22
Higdon J.C., Lingenfelter R.E., 1990, ARA&A 28, 401
Hurley K., 1988, Cosmic Gamma Rays, Neutrinos and Related Astrophysics, in: Shapiro M., Wefel J. (eds.) NATO ASI Series C270. Kluwer, Dordrecht, p. 337
Klebesadel R.N., Strong I.B., Olson R.A., 1973, ApJ 182, L85
Liang E.P., Petrosian V. (eds.), 1986, Gamma Ray Bursts, AIP Conference Proc. No. 141, American Institute of Physics, New York
Manchester R.N., Taylor J.H., 1981, AJ 86, 1953
Marar T.M.K., Sharma M.R., Seetha S., et al., 1994, A&A, this issue
Meegan C.A., Fishman G.J., Wilson R.B., et al., 1992, Nat 305, 143
Winckler J.R., Bhavsar P.D., Anderson K.A., 1962, J. Geophys. Res. 67, 3717

© European Southern Observatory • Provided by the NASA Astrophysics Data System